Available online at www.sciencedirect.com
ScienceDirect
Geochimica et Cosmochimica Acta 70 (2006) 5601–5616
Geochimica
www.elsevier.com/locate/gca

Correlated microanalysis of zircon: Trace element, $\delta^{18}O$, and U–Th–Pb isotopic constraints on the igneous origin of complex >3900 Ma detrital grains

Aaron J. Cavosie [a,*], John W. Valley [b], Simon A. Wilde [c], E.I.M.F. [1]

[a] Department of Geology, University of Puerto Rico, Mayagüez, PR 00681, USA
[b] Department of Geology and Geophysics, University of Wisconsin, Madison, WI 53706, USA
[c] Department of Applied Geology, Curtin University of Technology, Perth, WA, Australia

Received 8 November 2005; accepted in revised form 14 August 2006

Abstract

The origins of >3900 Ma detrital zircons from Western Australia are controversial, in part due to their complexity and long geologic histories. Conflicting interpretations for the genesis of these zircons propose magmatic, hydrothermal, or metamorphic origins. To test the hypothesis that these zircons preserve magmatic compositions, trace elements [rare earth elements (REE), Y, P, Th, U] were analyzed by ion microprobe from a suite of >3900 Ma zircons from Jack Hills, Western Australia, and include some of the oldest detrital zircons known (4400–4300 Ma). The same ~20 μm domains previously characterized for U/Pb age, oxygen isotope composition ($\delta^{18}O$), and cathodoluminescence (CL) zoning were specifically targeted for analysis. The zircons are classified into two types based on the light-REE (LREE) composition of the domain analyzed. Zircons with Type 1 domains form the largest group (37 of 42), consisting of grains that preserve evolved REE compositions typical of igneous zircon from crustal rocks. Grains with Type 1 domains display a wide range of CL zoning patterns, yield nearly concordant U/Pb ages from 4400 to 3900 Ma, and preserve a narrow range of $\delta^{18}O$ values from 4.7‰ to 7.3‰ that overlap or are slightly elevated relative to mantle oxygen isotope composition. Type 1 domains are interpreted to preserve magmatic compositions. Type 2 domains occur in six zircons that contain spots with enriched light-REE (LREE) compositions, here defined as having chondrite normalized values of $La_N > 1$ and $Pr_N > 10$. A subset of analyses in Type 2 domains appear to result from incorporation of sub-surface mineral inclusions in the analysis volume, as evidenced by positively correlated secondary ion beam intensities for LREE, P, and Y, which are anti-correlated to Si, although not all Type 2 analyses show these features. The LREE enrichment also occurs in areas with discordant U/Pb ages and/or high Th/U ratios, and is apparently associated with past or present radiation damage. The enrichment is not attributed to hydrothermal alteration, however, as oxygen isotope ratios in Type 2 domains overlap with magmatic values of Type 1 domains, and do not appear re-set as might be expected from dissolution or ion-exchange processes operating at variable temperatures. Thus, REE compositions in Type 2 domains where mineral inclusions are not suspected are best interpreted to result from localized enrichment of LREE in areas with past or present radiation damage, and with a very low fluid/rock ratio. Correlated *in situ* analyses allow magmatic compositions in these complex zircons to be distinguished from the effects of secondary processes. These results are additional evidence for preservation of magmatic compositions in Jack Hills zircons, and demonstrate the benefits of detailed imaging in studies of complicated detrital zircons of unknown origin. The data reported here support previous interpretations that the majority of >3900 Ma zircons from the Jack Hills have an origin in evolved granitic melts, and are evidence for the existence of continental crust very early in Earth's history.

1. Introduction

Studies of detrital zircons with ages from 4400 to 3900 million years (Ma) have greatly contributed to our understanding of the evolution of the early Earth (e.g. Froude

* Corresponding author. Fax: +1 787 265 3845.
E-mail address: acavosie@uprm.edu (A.J. Cavosie).
[1] Edinburgh Ion Microprobe Facility, School of Geosciences, University of Edinburgh, Edinburgh, Scotland, UK.

0016-7037/$ - see front matter © 2006 Elsevier Inc. All rights reserved.
doi:10.1016/j.gca.2006.08.011

et al., 1983; Compston and Pidgeon, 1986). While no intact rocks older than 4030 Ma are known (Bowring and Williams, 1999), the chemical compositions of these detrital grains have been used to make inferences about the composition, petrogenesis, and geologic history of the original host rocks to the zircons, which provide insights into geological processes on the early Earth (Maas et al., 1992; Amelin et al., 1999; Mojzsis et al., 2001; Peck et al., 2001; Wilde et al., 2001; Valley et al., 2002; Cavosie et al., 2004; Turner et al., 2004; Cavosie et al., 2005; Crowley et al., 2005; Harrison et al., 2005; Watson and Harrison, 2005; Iizuka et al., 2006).

The assumption that these zircons preserve magmatic compositions is implicit in making inferences about igneous host rocks and geologic processes at that time. However, many of these zircons are complicated and the identification of a small, but significant number of >3900 Ma grains with complex age spectra (Nelson et al., 2000; Mojzsis et al., 2001; Peck et al., 2001; Wilde et al., 2001; Nelson, 2002; Cavosie et al., 2004; Wyche et al., 2004), disturbed internal zoning in cathodoluminescence (CL) (Nelson et al., 2000; Cavosie et al., 2004; Nemchin et al., 2006), and suspected non-magmatic $\delta^{18}O$ values (Cavosie et al., 2005) demonstrates that some zircons with altered chemical compositions occur in the >3900 Ma population. Furthermore, internal complexity, present in some zircons, suggests that alteration may be localized, such that individual crystals contain domains that are well preserved along with domains that are altered (Valley et al., 2006). The number of altered zircons in any sample set depends on the post-igneous and sedimentary history, and also on unavoidable sorting during sample preparation. Given their demonstrated grain-scale complexities, if we are to determine their origin these early Archean zircon populations require detailed imaging and high spatial resolution *in situ* techniques.

The goal of this study is to determine if the trace-element abundances in early Archean detrital zircons from the Jack Hills, Western Australia preserve magmatic compositions (e.g. Maas et al., 1992; Peck et al., 2001; Wilde et al., 2001; Cavosie et al., 2004), or are the result of non-magmatic processes (Whitehouse and Kamber, 2002; Hoskin, 2005; Nemchin et al., 2006). Uncertainty exists concerning the genesis of these rare zircons (i.e. magmatic, hydrothermal, metamorphic), the tectonic setting of their parent melts (meteorite impact, plume, subduction, or deep burial), host rock composition (felsic vs. mafic), and degree of igneous differentiation (primitive vs. evolved). The documentation of what constitutes preserved magmatic trace-element compositions in >3900 Ma igneous zircons will provide additional geochemical evidence on the nature of early Archean processes that created the zircon-bearing melts. Trace-element compositions [e.g. the rare earth elements (REE), P, Y, Th, U] were determined for 82 spots from a population of forty-two 4400 to 3900 Ma detrital zircons. The same grain domains previously interpreted to preserve magmatic compositions (Cavosie et al., 2004, 2005) were specifically targeted for *in situ* analysis in order to correlate closely the trace-element data with the results of prior U/Pb and $\delta^{18}O$ analyses, and also CL imaging. The protocol of making all analyses on a single spot is necessary to place better constraints on the range of primary compositions preserved in these zircons.

2. Trace elements in zircon

2.1. Overview

Zircon incorporates a wide range of trace elements within its crystal structure, and these have been used to infer a diverse range of petrogenetic processes (Speer, 1982; Belousova et al., 2002; Finch and Hanchar, 2003; Hoskin and Schaltegger, 2003; Watson and Harrison, 2005). Although multiple analytical methods are available for the study of elements at trace levels in zircon, only *in situ* methods [e.g. secondary ion mass spectrometry (SIMS) and laser ablation inductively coupled plasma mass spectrometry (LA-ICPMS)] are sensitive to elements present at sub-ppm levels, and are able to avoid visible surface inclusions, cracks, radiation damaged zones, and other imperfections that can affect the analysis (Hinton and Upton, 1991; Hoskin, 1998). In this study, >3900 Ma detrital zircons were analyzed *in situ* by SIMS, as bulk methods would mix data from different age populations, and SIMS analytical spots are typically smaller than laser ablation spots for a given precision. Accordingly, we compare our results primarily with the findings of other *in situ* studies.

2.2. Rare earth elements (REE) in zircon

The decreasing ionic radii of the REE with increasing atomic number results in partitioning behavior that imparts characteristic patterns to chondrite normalized values in zircon (e.g. Hinton and Upton, 1991; Maas et al., 1992; Hoskin, 1998; Hoskin and Ireland, 2000; Belousova et al., 2002; Hoskin and Schaltegger, 2003). The main feature of a 'typical' pattern for igneous zircon is increasing enrichment in trivalent REEs from La to Lu, owing to the increasing compatibility of the smaller ionic radii REE in zircon. Other features include a positive Ce anomaly from incorporation of Ce^{+4} [denoted as Ce/Ce*, where Ce is the chondrite normalized value and $Ce^* = (La_{ppm} \times Pr_{ppm})^{1/2}$], and a negative Eu anomaly from the depletion of Eu^{2+} [denoted as Eu/Eu*, where Eu is the chondrite value and $Eu^* = (Sm_{ppm} \times Gd_{ppm})^{1/2}$] (Hoskin and Schaltegger, 2003).

The main mechanism for the incorporation of REE in zircon is commonly assumed to be 'xenotime-type' substitution, where $(Y + REE)^{3+} + P^{5+} = Zr^{4+} + Si^{4+}$, maintaining charge balance (Hinton and Upton, 1991; Hoskin et al., 2000; Finch et al., 2001; Hoskin and Schaltegger, 2003). Due to similar ionic radius and charge, Y partitioning in zircon closely approximates Ho (Hinton and Upton, 1991;

Hinton, 1996), and therefore plays an important role in 'xenotime-type' substitution. If the incorporation of REEs is governed solely by 'xenotime-type' substitution, the atomic ratio for (Y + REE)/P should be close to 1. Observations of (Y + REE)/P ratios >1 are evidence of additional substitutions or alternative processes that incorporate REEs in zircon (Hoskin et al., 2000; Finch et al., 2001; Hoskin and Schaltegger, 2003; Tomaschek et al., 2003; Spandler et al., 2004; Rayner et al., 2005). REE substitutions that do not involve P have also been investigated (Finch et al., 2001; Finch and Hanchar, 2003; Hinton et al., 2003).

Specific characteristics of REE abundances and/or patterns have been proposed for distinguishing zircon from different geologic environments, providing a framework for interpreting trace-element data in detrital grains of unknown origin. Belousova et al. (1998, 2002) proposed that mantle zircons can be discriminated from crustal zircons by the overall low abundance of REE (e.g. $<\sim$50 ppm). Hoskin and Ireland (2000) noted that crustal zircons from a wide-range of igneous rock compositions have few distinguishing characteristics in REE patterns. Variations in Ce and Eu anomalies have also been interpreted as reflecting zircon crystallization under specific conditions. Zircons that lack a positive Ce anomaly are known only from Lunar samples formed under relatively reducing conditions (Ireland and Wlotzka, 1992), while zircons that lack a negative Eu anomaly have been interpreted as forming in plagioclase-absent assemblages, including kimberlite and syenite (Belousova et al., 1998) and eclogites (Rubatto, 2002; Bingen et al., 2004).

2.3. Prior trace-element studies on >3900 Ma detrital zircons

Previous studies of >3900 Ma zircons have reported most REE patterns with the typical characteristics of igneous zircon described above (Maas et al., 1992; Peck et al., 2001; Wilde et al., 2001; Crowley et al., 2005). A small number of grains have also been reported with unusual enrichments in LREEs, with abundances ranging from 10 to 100 s times chondritic values, and flatter REE patterns from La through Nd (Maas et al., 1992; Peck et al., 2001; Wilde et al., 2001). The overall enrichment and anomalies in the REEs have been interpreted to be a consequence of zircon crystallization in fractionated melts, consistent with the existence of differentiated rocks on the early Earth (Maas et al., 1992; Peck et al., 2001; Wilde et al., 2001). However, unusually high LREE enrichment in Jack Hills zircons has also been interpreted to be the result of non-magmatic processes (Whitehouse and Kamber, 2002; Hoskin, 2005; Nemchin et al., 2006). Here, we document the REE abundances in a diverse group of Jack Hills zircons previously characterized by other geochemical criteria as magmatic (or otherwise) in order to address the different interpretations for their origin.

3. Samples and methods

3.1. Jack Hills detrital zircons

The detrital zircons analyzed for trace elements are from the Jack Hills, Western Australia, and have previously been characterized for U–Pb age, CL pattern, $\delta^{18}O$, mineral inclusions, and other physical grain aspects (Peck et al., 2001; Wilde et al., 2001; Cavosie et al., 2004, 2005). Two zircons previously analyzed for trace elements (Peck et al., 2001; Wilde et al., 2001) were re-analyzed in this study. The zircons are from metasedimentary samples W74, 01JH36, 01JH54, and 01JH60 (Wilde et al., 2001; Cavosie et al., 2004). The zircons range in age from 4400 to 3900 Ma, with the majority interpreted as preserving magmatic compositions based on nearly concordant U–Pb ages ($\geqslant$85%), Th–U ratios (0.06–1.79), preserved growth zoning in CL, and $\delta^{18}O$ values (5.3–7.3‰). A few grains (or grain domains) were previously interpreted as altered based on anomalous values of one or more of the above criteria (Cavosie et al., 2004, 2005). Zircon domains that are $\geqslant$85% concordant preserve primary isotopic information, whereas open-system behavior in both the U–Pb and Th–U systems was demonstrated for zircon domains $<\sim$85% concordant (Cavosie et al., 2004).

Previous ion microprobe analyses for $\delta^{18}O$ were made in the same location (or nearly so) as the age analyses (Cavosie et al., 2005). It is assumed that implanted ^{16}O from the U–Pb analysis could affect subsequent analysis of $\delta^{18}O$, and for this reason the $\delta^{18}O$ analyses were made on re-ground and re-polished surfaces with the prior ion microprobe pits removed (see analytical details in Cavosie et al., 2005). However, ion implantation during a SIMS analysis is very shallow and much of the implanted ^{16}O would be removed by pre-sputtering, so it is not known if this precaution is necessary. The range in $\delta^{18}O$ values for this suite of samples is from 3.9‰ to 18.4‰, however post-analysis SEM imaging revealed that many of the anomalous $\delta^{18}O$ analyses were located on cracks or in damaged grain areas, and are interpreted as 'unreliable' based on differences in sputtering behavior between these analyses and the standard grains (Cavosie et al., 2005). When the above 'unreliable' analyses ($\sim$33% of all analyses) are excluded, the range in values from concordant domains is 4.6‰ to 7.3‰, with one outlier at 10.3‰ (Peck et al., 2001; Wilde et al., 2001; Cavosie et al., 2005).

3.2. Zircon standards 91500, CZ3, and KIM-5

Three zircon standards were analyzed for selected trace elements. Zircon standard 'Geoscience 91500' (hereafter '91500') is a 'multiple-use' standard, and has been characterized for trace-element abundance (e.g. REE, P, Y and others), isotopic composition (Lu–Hf), age (U–Th–Pb), and $\delta^{18}O$ (Wiedenbeck et al., 2004). Zircon standard KIM-5 is used as an oxygen isotope standard

(Valley, 2003), and has also been characterized for Hf content (Peck et al., 2001) and U–Th–Pb age (Cavosie et al., 2005), but not previously for REE. Zircon standard CZ3 is used as a U/Pb standard in geochronological studies by the Western Australian SHRIMP Consortium, with established values for both U–Pb and Th–U ratios (Pidgeon et al., 1994) and Hf content (Wu et al., 2006), but has not previously been characterized for REE.

The three standards have quite different apparent origins, and represent zircons from both crustal (91500, CZ3) and mantle (KIM-5) environments. Zircon 91500 is a megacryst from a metamorphosed syenite complex in Ontario, Canada, although its exact host rock is unknown (Wiedenbeck et al., 2004). CZ3 is a detrital megacryst from Sri Lanka (Nasdala et al., 2004), and is suspected to have originated in pegmatite, although its host rock is also unknown. KIM-5 is a megacryst from a South African kimberlite (Valley et al., 1998; Valley, 2003; Cavosie et al., 2005).

3.3. Ion microprobe analytical conditions

Zircons were analyzed for trace elements using a CAMECA ims-4f ion microprobe at the University of Edinburgh. The analyses followed analytical methods described previously (e.g. Hinton and Upton, 1991). A primary $^{16}O^-$ beam with a current of 12 nA and a 10 kV accelerating voltage was defocused to a ~20 μm diameter spot, producing circular craters that are roughly 6–8 μm deep. A 120 eV offset was applied, with secondary ions selected from a 40 eV energy window. Secondary ions were extracted at 4380 kV and energy filtering reduced molecular interferences. The mass resolving power recorded at low mass resolution was >500, thereby resolving unit masses at all masses analyzed. Ions were counted with a single electron multiplier detector (EM) using magnetic peak switching. Ten cycles of measurements were made during an analysis. The counting time for each mass varied from 2 s for major and minor elements (e.g. Si and Hf) to 15 s for the background and the LREE (e.g. La and Pr). Together with peak switching, the total analysis time per spot was ~40 min.

Elemental abundances were normalized to total Si assuming 15.0 wt% for zircon (which yields a maximum error of up to 3% (relative) for trace elements due to variation of 0.5 wt% Si), and calibrated with NIST SRM610 (using values of Pearce et al., 1997). Each analysis of NIST SRM610 was followed by an analysis of 91500, which served as a second REE standard, or 'monitor', during the analytical sessions.

The following run table was employed in each zircon analysis, and includes 23 masses for counting elements of interest and also evaluating background and molecular interferences: ^{30}Si, ^{31}P, $^{44}(^{28}Si^{16}O)$, ^{89}Y, $^{130.5}$Bkg, ^{134}(ZrSiO), ^{139}La, ^{140}Ce, ^{141}Pr, ^{143}Nd, ^{149}Sm, ^{151}Eu, ^{157}Gd, ^{159}Tb, ^{161}Dy, ^{165}Ho, ^{167}Er, ^{169}Tm, ^{172}Yb, ^{175}Lu, ^{177}Hf, ^{232}Th, ^{238}U. A comprehensive list of isotopes/elements with interference corrections (isobars listed in parentheses) includes: ^{31}P ($^{30}Si^{1}H$), ^{151}Eu ($^{135}Ba^{16}O$), ^{157}Gd ($^{141}Pr^{16}O$), ^{159}Tb ($^{143}Nd^{16}O$), ^{161}Dy ($^{145}Nd^{16}O$), ^{167}Er ($^{151}Eu^{16}O$), ^{172}Yb ($^{156}Gd^{16}O$, $^{156}Dy^{16}O$), ^{175}Lu ($^{159}Tb^{16}O$), ^{177}Hf ($^{161}Dy^{16}O$). By applying an energy offset of 120 eV, the corrections for ^{151}Eu, ^{157}Gd, ^{161}Dy, ^{167}Er, ^{172}Yb, ^{175}Lu, and ^{177}Hf are nearly negligible in the case of zircon. The rest of the corrections were made on-line using the data reduction program JCION5 at the University of Edinburgh Ion Microprobe Facility.

Aberrant 'spikes' corresponding to ~30–45 ion counts appeared during some analyses. The aberrant counts appeared as a 2–3 cps 'spike' for elements with a count time of 15 s, a 3–4 cps 'spike' for elements with a count time of 10 s, and so on. Aberrant spikes were only detectable and significant during the counting of low abundance elements for most of the zircon samples (e.g. La, Pr, Nd, Sm, Eu, and Bkg), but were also identified for Tb, Ho, Tm, and Yb in zircons with low abundances of HREE. Aberrant 'spikes' were not detected for the major or minor elements (e.g. Si, P, Hf, and Y). Spikes, if present, typically appeared during one of the counting cycles for one or more elements during an analysis. Every analysis was reviewed 'off-line' for the presence of these 'spikes', and they were removed only when the 'spike' matched the predicted magnitude of 30–45 counts (see above). A new cps value was then assigned to the cycle that contained the spike by taking the average of the count rate for the cycles on either side of the spike. The cause of the spikes was later found to be related to an external voltage discharge that was detected by the EM (J. Craven, 2005, personal communication).

3.4. Analysis strategy

Images of the 42 zircon crystals in cathodoluminescence (CL), complete with REE, $\delta^{18}O$, and U–Pb analytical spots are shown in Fig. 1. Trace-element analyses were made in the pits where $\delta^{18}O$ was previously measured, and below the surface where U–Th–Pb isotopic data were collected on a prior polished surface (see example in Fig. 2). With careful beam positioning, this strategy allows analysis of REEs in concordant U–Pb domains in crystals with inherited cores, variable zoning, inclusions, or radiation damage (Fig. 2a). However in some cases, the REE analyses were later found by post-analysis SEM imaging to have only partially overlapped or, in some cases, entirely missed the targeted area (see examples in Fig. 1).

Comparative measurements (tests) were conducted to evaluate the quality of trace-element analyses made in the bottom of pits previously implanted with cesium during $\delta^{18}O$ analysis (Fig. 2b). Back-to-back analyses of 91500 were made on a fresh surface (i.e. without implanted Cs) and in a $\delta^{18}O$ pit (i.e. a surface with implanted Cs) on three separate occasions during the analytical sessions. No significant differences in REE abundance were observed, demonstrating that trace-element data collected within $\delta^{18}O$ analysis pits were not

affected by the presence of shallowly implanted cesium (see test pairs in electronic annex EA-1).

4. Results

4.1. Zircon standards

Elemental abundances for the zircon standards are presented in EA-1. Chondrite normalized rare earth element plots for the standards [using chondritic values of McDonough and Sun (1995)] are displayed in Fig. 3. Nine analyses were made on a single grain of 91500 (Fig. 3a). Elements present at >1 ppm levels show good reproducibility (3–20%, relative), while large variations (50–90%) occurred in elements present at sub-ppm levels (e.g. La, Pr, and Nd). Two analyses of CZ3 made on different grains show similar reproducibility for most elements above 1 ppm (3–15%), again with the most variability (35–90%) observed in low abundance elements (e.g. La, Pr, Nd, and Eu) (Fig. 3b). Three analyses of one grain of KIM-5 show the most variability, between 10% and 60% for all elements except P, which is attributed to the very low overall abundance of trace elements in KIM-5 (Fig. 3c).

The total REE (in ppm) varies significantly for the three standards, decreasing from 157 in 91500, to 46 in CZ3, and 19 in KIM-5. Average normalized REE patterns demonstrate similarities and differences amongst the three zircons (Fig. 3d). The relative abundance of LREEs is similar for all three, with $(Sm/La)_N$ ranging from 17.9 in 91500 to 3.1 in CZ3. Differences in HREE abundance are reflected in variable $(Yb/Sm)_N$

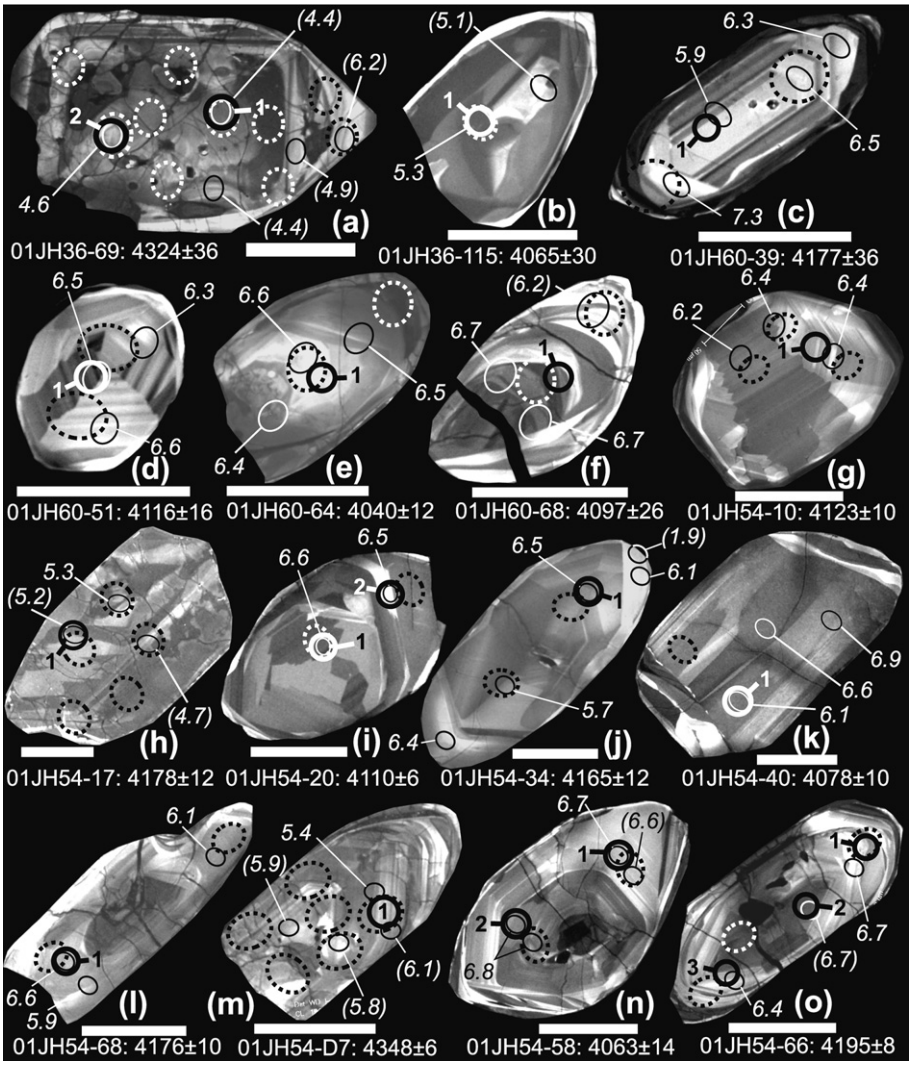

Fig. 1. Cathodoluminescence (CL) images of >3900 Ma detrital zircons from Jack Hills, complete with trace element, $\delta^{18}O$, and U–Pb analysis locations (refer to 'key' at bottom of figure). The oldest concordant age is given in Ma (±2 SD) below the scale bar. Trace element analyses are numbered 1, 2, 3, . . . , n. All $\delta^{18}O$ values are vs. VSMOW. U–Pb ages are in Ma. Values in parentheses indicate analyses where U–Pb or $\delta^{18}O$ data were rejected. See text for discussion. (Note: U–Pb spots for grains (p) and (u) are not labeled for clarity [see Peck et al., 2001 and Cavosie et al., 2004] for U–Pb spot locations for these grains). Scale bars are all 100 μm.

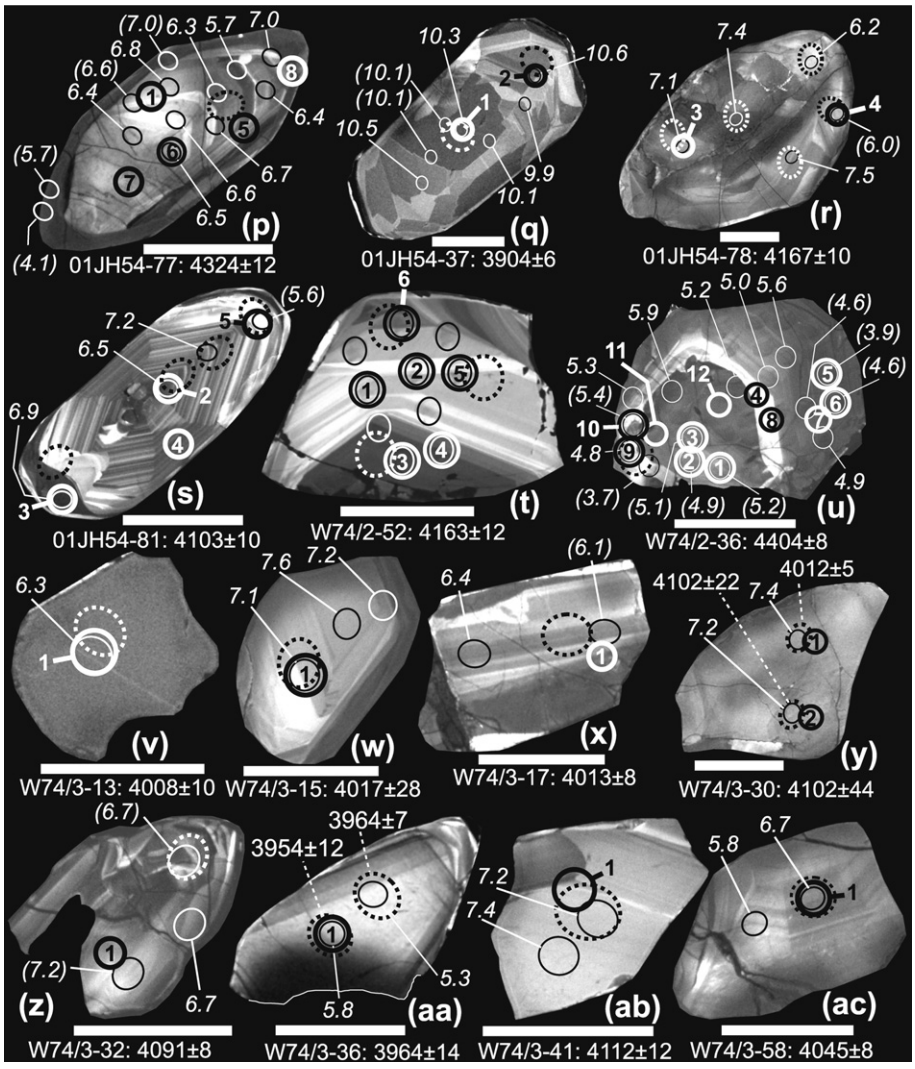

Fig. 1 (*continued*)

values, from 126.6 in 91500 to 5.1 in KIM-5. The Ce anomaly (Ce/Ce*) is highest in 91500 (18.4), and more subdued in KIM-5 (2.5) and CZ3 (1.0). The Eu anomaly (Eu/Eu*) is comparatively small in all three standards, from 0.7 to 1.1, indicating all three zircons crystallized in environments relatively undepleted in Eu^{2+}.

Average values of Th and U (in ppm), and the Th–U ratio listed in the form (x, y, z) are (31, 99, 0.32) for 91500, (31, 658, 0.05) for CZ3, and (2, 8, 0.24) for KIM-5 (EA-1), and are in good general agreement with previous studies (91500: Wiedenbeck et al., 2004; KIM-5: Cavosie et al., 2005). The notable exception is the U concentration of 658 in CZ3, which is higher than the range of 530–560 ppm reported by Pidgeon et al. (1994).

Abundance of P (ppm) is a factor of two higher in KIM-5 (51.7) and CZ3 (45.7), compared to 91500 (24.9), whereas the relative abundances of Y are reversed, with the highest value in 91500 (146.4) and lower values in CZ3 (67.6) and KIM-5 (32.3) (EA-1). The three standards have notably different (Y + REE)/P atomic ratios, ranging from 0.29 for KIM-5, to 3.20 for 91500 (Fig. 4a). The positive correlation of (Y + REE)/P with total REE for these zircons and 54 other kimberlite zircons (Fig. 5) suggests that complex 'xenotime-type' substitution requires REE abundances in excess of 50 ppm, and may only occur in crustal zircons. The trace element results for KIM-5 and 91500 are consistent with an origin for the two grains in the mantle (e.g. kimberlite) and crust (e.g. syenite), respectively. The origin of CZ3 based on the REE data is less clear. The small Eu anomaly (Eu/Eu* = 1.1), low total REEs (46 ppm), and similarity to kimberlitic zircons (Fig. 5) is more consistent with an origin in a mantle-derived melt, however the high U concentration (658 ppm) and resultant low Th–U ratio (0.05) are not typical features of mantle zircon.

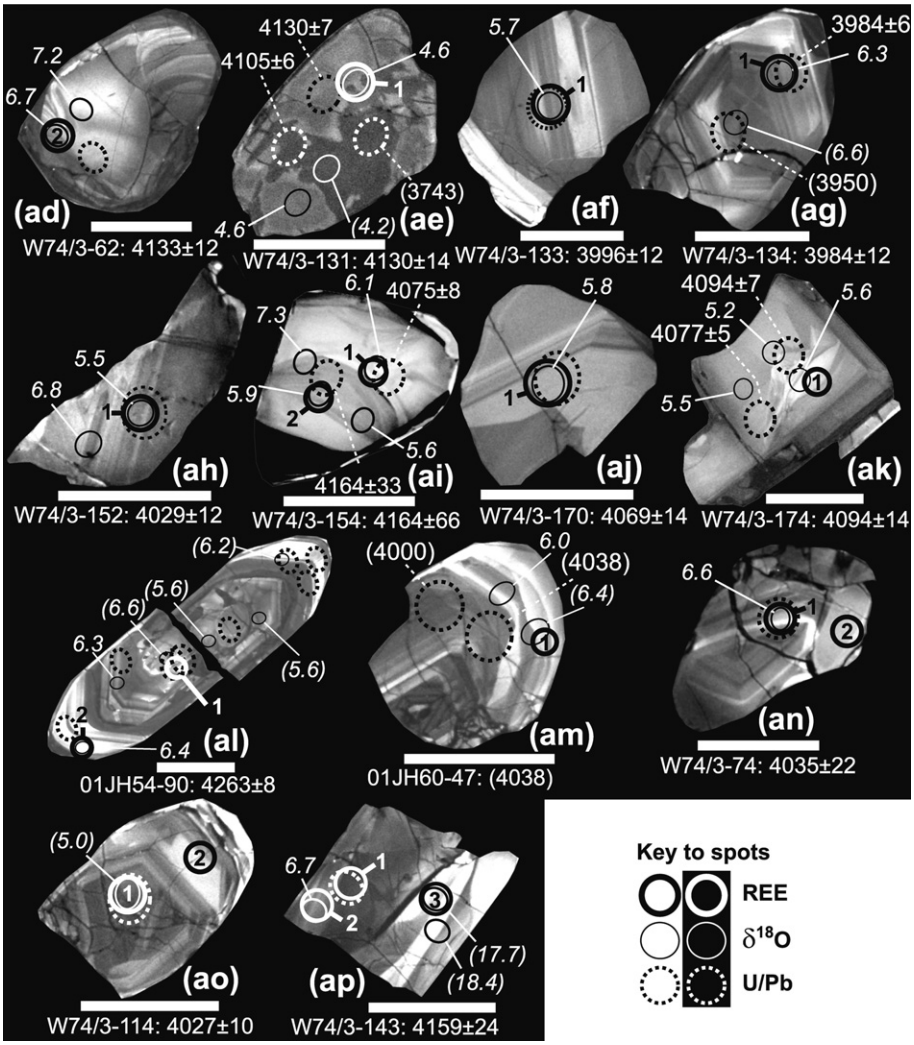

Fig. 1 (*continued*)

4.2. The Jack Hills zircons: Two types of REE pattern

Elemental abundances for 79 of 82 analyses of selected trace elements in 42 Jack Hills zircons are listed in electronic annex EA-2 (three analyses that partially overlapped on epoxy were discarded), and chondrite normalized REE plots are displayed in Fig. 6. The data can be classified into two different types (Type 1 and Type 2) to facilitate evaluation of REE patterns between different samples, and also for evaluating the population as a whole. Fig. 6a–g display REE patterns with overall characteristics typical of crustal magmatic zircon (e.g. Hoskin and Ireland, 2000), and are here classified as 'Type 1' REE patterns. Type 1 patterns represent the majority of the analyses, and include data from 37 of the 42 (88%) grains analyzed.

Fig. 6(h) displays 'Type 2' patterns. These are enriched in the LREE relative to Type 1 patterns, here defined as having both $La_N > 1$ and $Pr_N > 10$. The Type 2 group consists of 15 analyses made on 6 grains. An important point to note is that the Type 1 and Type 2 classification refers to REE patterns for spot analyses within a grain domain, and not necessarily to entire grains, as at least one zircon grain contains both types of pattern (W74/2-36). Detailed characteristics of the two groups are discussed in the following sections (Note: the Type 1 and Type 2 classifications described here, although defined differently, are broadly similar to the Type 1 and Type 2 classifications of Hoskin, 2005).

4.3. Jack Hills zircons with Type 1 REE patterns

Grains with Type 1 patterns show similar characteristics. Values of $(Sm/La)_N$ range from 4.6 to 352.4, with an average of 78.8, while values of $(Yb/Sm)_N$ show a more restricted range, from 25.5 to 204.9 (avg. = 85.3). Values of Ce/Ce* range from 2.9 to 94.3 (avg. = 27.6), and Eu/Eu* range from 0.06 to 0.92 (the latter value from grain 01JH54-37, Fig. 6d), with an average of 0.24. Total REE abundance (ΣREE) ranges from 129 to 2611 ppm (avg. = 895 ppm). The above values are similar to averages reported for zircons from a wide compo-

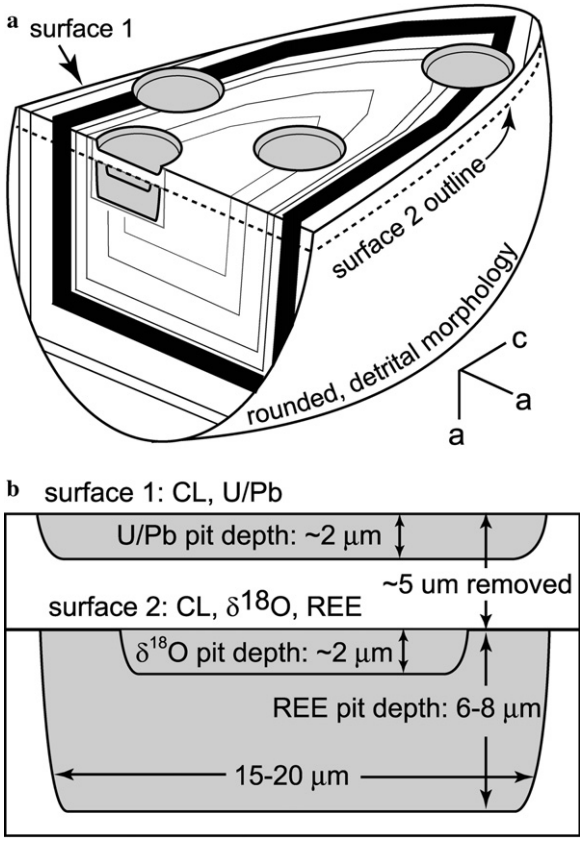

Fig. 2. (a) Schematic representation of a zoned detrital zircon with volume analyzed for U–Pb, $\delta^{18}O$, and REE (orientation of crystallographic axes are indicated to the lower-right). The 'a–c plane' [(100), roughly horizontal] represents polished surfaces 1 and 2. Surface 1 was analyzed for U–Pb (shaded ovals). The dashed line indicates the plane of surface 2, analyzed for $\delta^{18}O$ and REE. The 'a–a plane' [(001), roughly vertical] shows a hypothetical cross-section through the grain, and the volumes analyzed for U/Pb, $\delta^{18}O$ and REE. See text for discussion. (b) Cross-section (001) of the volumes analyzed for U–Pb age, $\delta^{18}O$, and REE in (a). The dimension of the entire volume varies, but is on average 20 µm in diameter, and 10–15 µm deep.

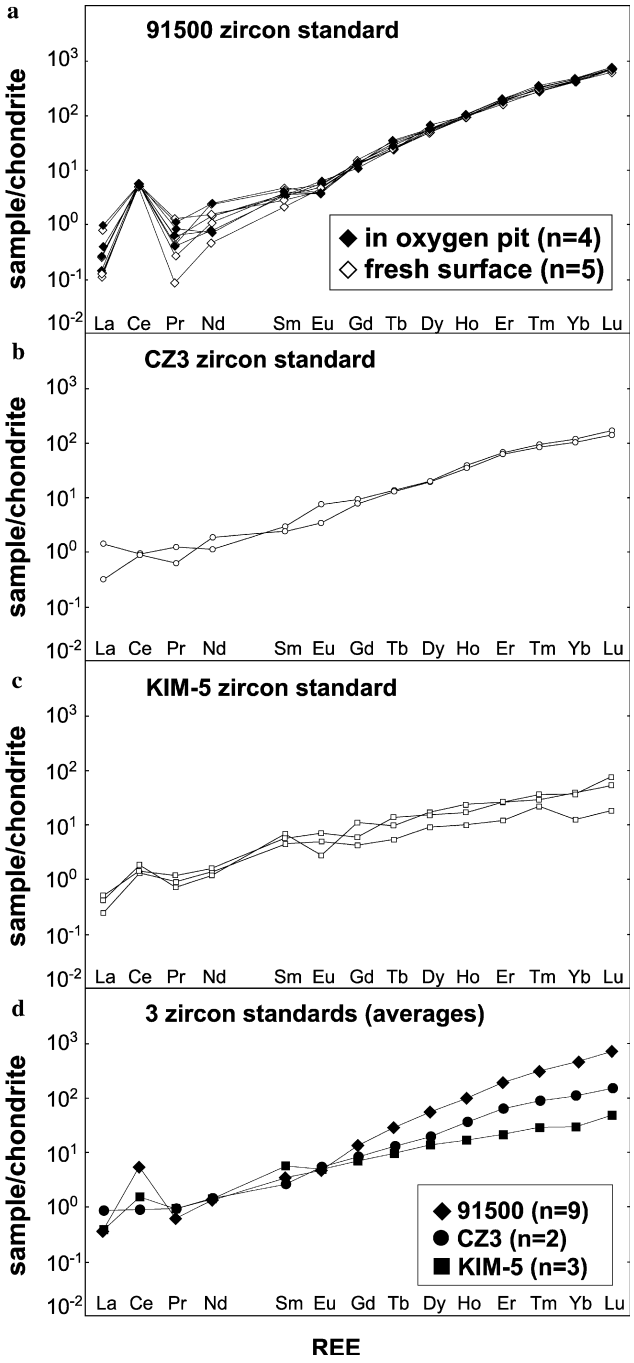

Fig. 3. Chondrite normalized REE plots of zircon standards. (a) Zircon standard 91500; (b) Zircon standard CZ3; (c) Zircon standard KIM-5; (d) Average values for each zircon standard.

sitional range of crustal igneous rocks (Hoskin and Schaltegger, 2003).

The Type 1 group shows a range of (Y + REE)/P atomic ratios from 0.87 to 3.91 (Fig. 4b; EA-2), indicating that normal 'xenotime-type' substitution is not the only mechanism for incorporation of REE in these grains. Several Type 1 analyses with (Y + REE)/P ratios ~3 (Fig. 4b) were made on zircons with previously identified phosphate inclusions, including apatite, xenotime, and monazite (Cavosie et al., 2004), which were avoided during analysis. Complex 'xenotime-type' substitutions require incorporation of additional charge balancing elements (Hoskin et al., 2000; Finch et al., 2001; Hanchar et al., 2001; Finch and Hanchar, 2003; Hinton et al., 2003), however the results of this study do not distinguish which specific complex 'xenotime-type' coupled substitution, if any, produced elevated (Y + REE)/P values in these Jack Hills zircons.

4.4. Jack Hills zircons with Type 2 REE patterns

The higher abundance of LREEs in Type 2 domains results in substantially lower $(Sm/La)_N$ values when compared to Type 1, ranging from 3.3 to 58.0 (avg. = 13.7). The HREE enrichment is also less pronounced, with values of $(Yb/Sm)_N$ from 3.6 to 67.4 (avg. = 27.1). Not surprisingly, Type 2 domains have noticeably smaller Ce anomalies, from Ce/Ce* = 2.0 to 10.3 (avg. = 4.2). The range of Eu anomalies is smaller

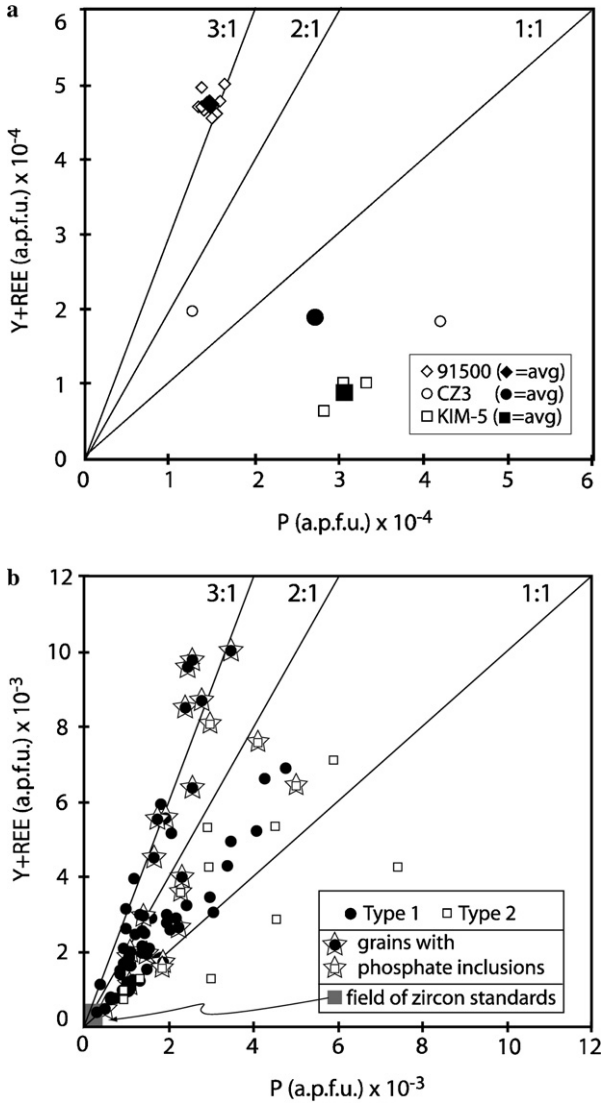

Fig. 4. Ratios of (Y + REE)/P in atoms per formula unit (a.p.f.u.). (a) Zircon standards. Open symbols are single analyses. (b) Jack Hills zircons. Stars are analyses on grains with exposed phosphate inclusions. These inclusions were avoided during analysis. Note that all standard data plot near the origin in (b), demonstrating the relative REE enrichment in Jack Hills detrital zircons. See text for discussion.

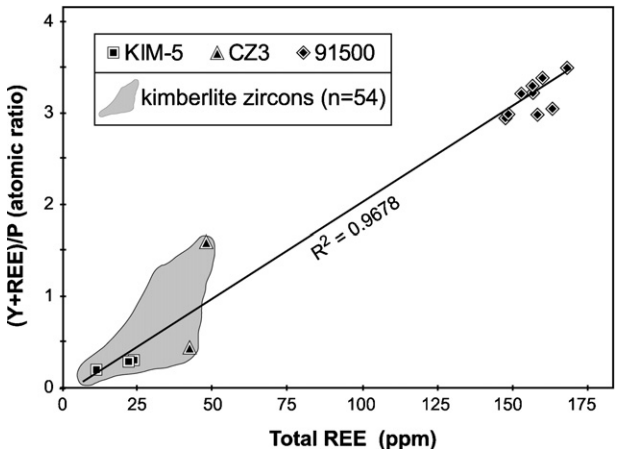

Fig. 5. Atomic ratio of (Y + REE)/P vs. total REE (in ppm) for zircons standards analyzed in this study. Field of kimberlite zircons defined from data of Belousova et al. (1998) ($n = 28$) and Spetsius et al. (2002) ($n = 26$). The linear regression includes all data, including the 54 kimberlite analyses. Note that both analyses of CZ3 lie within the kimberlite field.

than Type 1, with Eu/Eu* = 0.16–0.45, although the average value is similar (0.30). Type 2 domains also have a smaller range of ΣREE than the Type 1 group, from 164 to 2117 ppm, but with a higher average value (1183 ppm).

The range for atomic ratios of (Y + REE)/P is slightly lower in Type 2 domains than in Type 1, ranging from 0.42 to 2.70 (Fig. 4a), and again indicates multiple REE substitution mechanisms. The lowest sub-unity values of (Y + REE)/P for Jack Hills zircons occur in Type 2 domains, and range from 0.42 to 0.84.

A subset of five analyses made in Type 2 domains from three grains are further distinguished. Analyses from grains W74/3-74, W74/3-114 ($n = 2$), and W74/3-143 ($n = 2$) all display enrichment in the middle-REEs (MREEs), resulting in noticeably flatter REE patterns from Gd to Ho (Fig. 6h), and reduced values of $(Ho/Gd)_N$ (avg. = 2.28) compared to the Type 2 group average of 4.07. These five analyses also have higher values for Th (385 vs. 367 ppm), U (342 vs. 302 ppm), and P (637 vs. 571 ppm), but less Y (992 vs. 1313 ppm) compared to the Type 2 group averages (EA-2). In addition, analyses from grains W74/3-74 and W74/3-143 have fractionated Y/Ho ratios relative to other analyses on the same grains (EA-2).

5. Discussion

5.1. Type 1 REE domains: Correlations with age, $\delta^{18}O$, and CL zoning

The main goal of this study is to identify preserved magmatic compositions in >3900 Ma zircons by correlating trace element compositions with U–Pb age, $\delta^{18}O$, and CL zoning previously reported from the same grain domains (Peck et al., 2001; Wilde et al., 2001; Cavosie et al., 2004; Cavosie et al., 2005). The trace elements in Type 1 domains largely appear to be representative of 'crustal' magmatic zircon compositions as summarized by Hoskin and Ireland (2000) (Fig. 6). Variations in REE patterns from Type 1 domains (e.g. ΣREE, $(Sm/La)_N$, $(Yb/Sm)_N$, Ce/Ce*, Eu/Eu*) likely record differences in magma compositions and/or processes associated with zircon crystallization, and are within the range of average values for crustal zircons. Zircons in the Type 1 group show a variety of CL zonal patterns, from oscillatory through to unzoned, and yield nearly concordant U–Pb ages from 4400 to 3900 Ma. Type 1 domains have $\delta^{18}O$ values from 4.6‰ to 7.3‰ (with one outlier at 10.3‰), values within or slightly above the range of 4.7–5.9‰ for mantle equilibrated zircon (Valley, 2003) (EA-2).

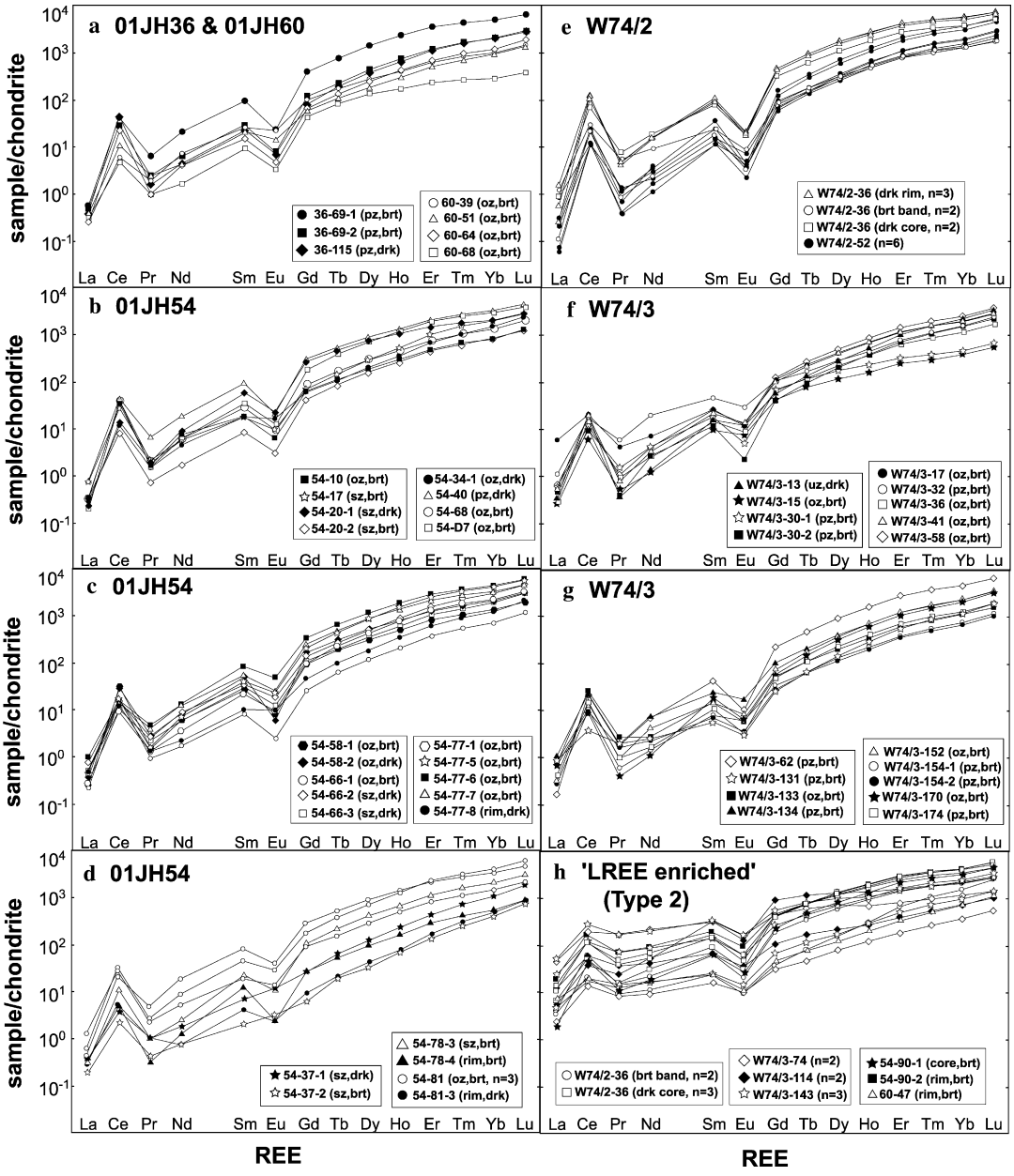

Fig. 6. Chondrite-normalized REE plots for 42 Jack Hills zircons. (a) Samples 01JH36 and 01JH60; (b–d) Sample 01JH54; (e) Sample W74/2; (f–g) Sample W74/3; (h) LREE 'enriched' (Type 2) patterns. (a–g) Type 1 patterns. See text for discussion.

The five highest ΣREE abundances in this study occur in Type 1 domains in grain W74/2-36 and 01JH36-69, both >4300 Ma. The overall shape of the high REE abundance patterns for these two grains is similar to typical Type 1 patterns (Fig. 6a and e). Both of these grains have oxygen isotope ratios that overlap with the mantle (e.g. $\delta^{18}O = 4.6 \pm 0.6‰$ and $5.4 \pm 0.8‰$, Cavosie et al., 2005) and contain quartz inclusions (Peck et al., 2001; Cavosie et al., 2004). There is no indication that the high REE abundance Type 1 domains in grains W74/2-36 and 01JH36-69 represent alteration, even though both of these grains contain fractures and have localized radiation damage, as evidenced by U–Pb discordance and high Th–U ratios in other areas of the grains (Wilde et al., 2001; Cavosie et al., 2004). The nine analyses in Type 1 domains of these two grains have Th–U ratios ranging from 0.51 to 0.84 (one at 1.79), and yield nearly concordant U–Pb ages. The Type 1 patterns in these grains are, therefore, interpreted as primary magmatic features, and given their ages, provide evidence for the origin of these zircons in quartz-saturated, REE-enriched magmas prior to 4300 Ma.

The following three grains are exceptions where the Type 1 trace-element pattern classification may not be a record of magmatic composition when all grain characteristics are considered. Analyses of rims were made on two grains, 01JH54-78 and 01JH54-81. The rim on grain 01JH54-78 is thin and brighter in CL than the core

(Fig. 1r), yields younger U–Pb ages, and a lower $\delta^{18}O$ value, whereas the rim on grain 01JH54-81 is darker in CL than the core (Fig. 1s), yields a younger U–Pb age, and has the same $\delta^{18}O$. The ΣREEs in both rims is lower than in their respective cores [01JH54-78: 212 (rim) vs. 816 ppm (core); 01JH54-81: 159 (rim) vs. 1258 ppm (core)], and the Y/Ho ratio in the rim of 01JH54-81 is fractionated relative to the core [33.8 (rim) vs. 24.0 (core)] (Fig. 6d, EA-2). Thus it is possible that sub-solidus modification resulted in REE depletion in the rims of these grains (Hoskin and Black, 2000; Tomaschek et al., 2003; Bingen et al., 2004; Spandler et al., 2004), including fractionating Y from Ho in the rim of grain 01JH54-81 (Hinton, 1996; Whitehouse and Platt, 2003).

Two analyses were made on grain 01JH54-37, a concordant 3900 Ma zircon with concentric oscillatory zoning that has been overprinted by asymmetric sector-zoning (Cavosie et al., 2004) (Fig. 1q). The two analyses yield nearly parallel REE patterns with overall low abundances (ΣREE = 129 and 361 ppm) (Fig. 6d), with the higher abundance in a dark CL sector (EA-2). Both analyses show only a weak negative Eu anomaly (Eu/Eu* = 0.88–0.92), the first time such a small anomaly has been documented in a ca. 3900 Ma zircon. While it is not known if recrystallization will 'erase' a pre-existing Eu anomaly, recrystallization does not appear to have affected the Eu anomaly of the rims of the two grains described previously. If magmatic in origin, the small Eu anomaly in grain 01JH54-37 indicates a largely unfractionated source relative to Eu, such as the mantle, an eclogite, or other plagioclase-poor environment. However, the unusually high $\delta^{18}O$ value of $10.3 \pm 0.6‰$ (2 SD, $n = 5$, Cavosie et al., 2005) for this grain is inconsistent with a mantle origin, and while formation in a ca. 3900 Ma eclogite is possible, no zircon from eclogite of any age is known with such high $\delta^{18}O$, and moreover this scenario is impossible to confirm. Several characteristics of grain 01JH54-37 bear striking resemblance to zircon standard 91500, including the small negative Eu anomaly (0.90 vs. 0.71), low average ΣREE abundance (245 vs. 157 ppm), Th/U ratio (0.38 vs. 0.32) and high $\delta^{18}O$ (10.3‰ vs. 9.9‰). While the overprinting of zonation seen by CL suggests a sub-solidus origin for these chemical compositions, the similarity of these distinctive characteristics allows for the possibility that grain 01JH54-37 may have formed in a ca. 3900 Ma syenite. Whatever its origin, it is thus far unique among ⩾3900 Ma zircons.

5.2. Type 2 domains: Evaluation of LREE enrichment

Type 2 domains show characteristics that lead us to conclude that LREE enrichment in these domains is not representative of magmatic composition (electronic annex EA-3). One outstanding question is the cause of the LREE enrichment. Prior explanations, including inadvertent analysis of LREE-bearing inclusions, complex REE substitution mechanisms, zircon-melt disequilibrium, and hydrothermal processes, are discussed below.

5.2.1. Analysis of LREE inclusions

Given the 6–8 μm depth of the REE analysis pit (Fig. 2), it is possible that LREE-bearing mineral inclusions (e.g. monazite and titanite) could have been incorporated into the analyzed volume. Grain surfaces were imaged pre-analysis with an SEM to avoid possible mineral inclusions, and none were identified associated with the Type 2 analyses during subsequent post-analysis SEM imaging. However, for 6 of the 15 Type 2 analyses, secondary ion beam intensities of LREE, Y, and P, (±Th, ±U), show an anti-correlation with Si over multiple cycles during a 10-cycle analysis (electronic annex EA-4a, -4b). The above observation indicates that several of the Type 2 analyses appear to have encountered sub-surface LREE-bearing inclusions during analysis. The compositions of the suspected inclusions are unknown, however the positive correlation of Y and P is indicative of xenotime (EA-4a, -4b) whereas the positive correlation of $(La/Sm)_N$ and Th (Fig. 7) for Type 2 analyses suggests that monazite may also have been analyzed (e.g. Whitehouse and Kamber, 2002). Titanite is another possible LREE-bearing mineral inclusion (e.g. Hoskin et al., 2000).

5.2.2. REE substitution mechanisms

Complex 'xenotime-type' substitutions, as evidenced by elevated (Y + REE)/P ratios, do not appear to be the cause of LREE enrichment for the samples in this study, as the range of (Y + REE)/P ratios in Type 2 domains (0.42–2.70) lies almost entirely within the range of Type 1 (0.87–3.91), which are not LREE enriched (Fig. 4b). Phosphorus abundance does appear to have some influence on the substitution mechanism(s), however, as the highest (Y + REE)/P values (e.g. >3) are found in domains with less than ~500 ppm P (Fig. 8). Domains with notably elevated P values (e.g. >~750 ppm) may have been enriched in P by secondary processes rather than through magmatic incorporation, as evidenced by the observation that five of

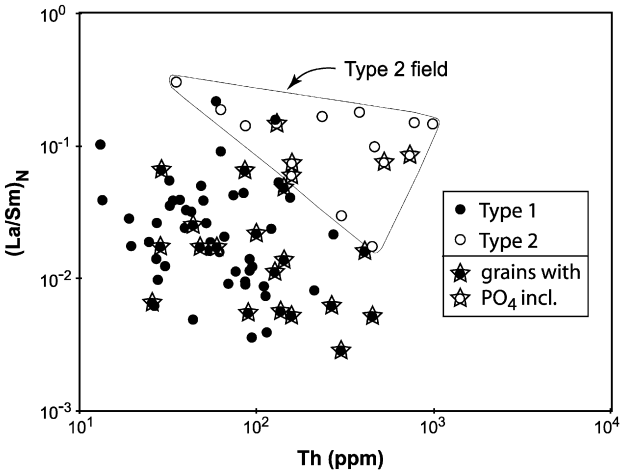

Fig. 7. Chondrite-normalized La/Sm values vs. total Th (in ppm) for Jack Hills zircons. The star symbols indicate an analysis made in a grain that contains known phosphate inclusions.

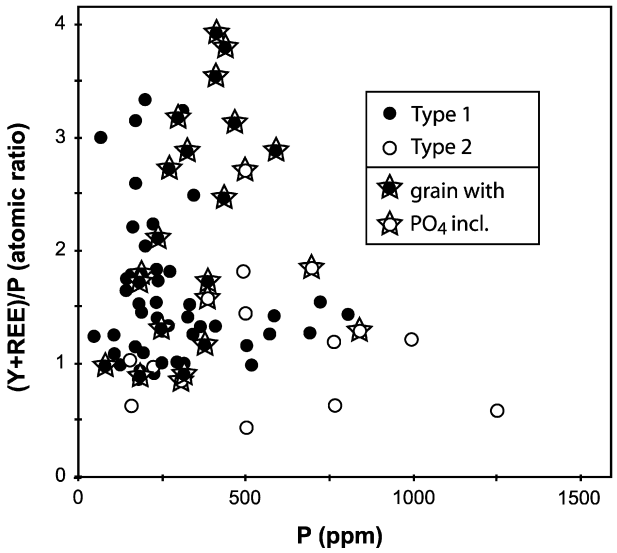

Fig. 8. Atomic ratios of (Y + REE)/P vs. P (in ppm) for Jack Hills zircons. Note that both the maximum (Y + REE)/P value and nearly all known phosphate inclusions occur in domains with <500 ppm P. Also note the decrease in (Y + REE)/P with increasing P (above 500 ppm) for Type 2 analyses. The star symbols indicate an analysis made in a grain that contains known phosphate inclusions.

the six zircons with known phosphate inclusions, which may have crystallized in phosphate-saturated magmas, all have <500 ppm P (Fig. 8).

5.2.3. LREE enrichment as a function of lattice damage

Type 2 domains have features indicative of alteration, including discordant U–Pb ages, high Th–U ratios, and disturbed CL zoning (EA-3). Type 2 domains are, therefore, areas that may have experienced radiation damage that is now annealed, thus it is possible that the REE composition of these domains is a result of the same processes that affected the U–Th–Pb systematics. A proposal

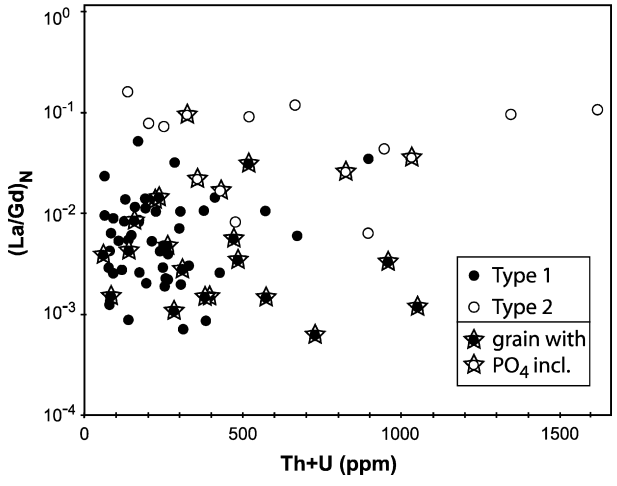

Fig. 9. Chondrite-normalized La/Gd values vs. total Th + U (in ppm) for Jack Hills zircons. The star symbols indicate an analysis made in a grain that contains known phosphate inclusions.

that the amount of LREE enrichment is proportional to the degree of lattice damage from alpha recoil by Whitehouse and Kamber (2002) was evaluated by plotting the combined U + Th content vs. $(La/Gd)_N$ (Fig. 9). Type 2 analyses show the highest $(La/Gd)_N$ values for any given U + Th concentration (Fig. 9), however, with the exception of two analyses above 1100 ppm, the range of Th + U abundance for all Type 2 domains is the same as for Type 1 domains, which do not show LREE enrichment (Fig. 9). Thus lattice damage (as inferred by present actinide abundance) does not appear to be the cause of the LREE enrichment.

5.2.4. Zircon-melt disequilibrium

Given that the zircons analyzed are detrital, it is not possible to evaluate hypothetical zircon-melt disequilibrium (Whitehouse and Kamber, 2002) until preserved samples of the protolith are identified.

5.3. Hydrothermal zircon

It has also been proposed that LREE enrichment is a common, possibly diagnostic feature of 'hydrothermal zircon', a general term used to describe zircon formed from or modified by fluids (Whitehouse and Kamber, 2002; Hoskin, 2005; Rayner et al., 2005). While the term hydrothermal has been loosely applied, it is important to distinguish zircons that were precipitated from a circulating hydrothermal fluid vs. those that have recrystallized or were altered in the presence of a high water activity pore fluid. Significantly, this pore fluid may be present at vanishingly low ratios of water:rock under effectively closed system conditions (i.e. little or no fluid movement into or out of the rock). Recognizing the need for a more precise working definition of 'hydrothermal zircon', Hoskin (2005) proposed three processes that can produce 'hydrothermal zircon', including precipitation from an aqueous fluid, dissolution–reprecipitation, and ion exchange with an aqueous fluid, however this definition does not provide a method for distinguishing hydrothermally precipitated zircon from igneous zircon altered by hydrous processes. These distinctions are significant, as dissolution–reprecipitation and precipitation processes appear to produce zircons with physical and chemical aspects that are distinct from magmatic zircon (e.g. Tomaschek et al., 2003), whereas characteristics of zircons affected by ion exchange with an aqueous fluid will likely depend on several factors, including the fluid volume and composition, and temperature and duration of alteration, and may not always produce a diagnostic signature.

To explore the possibility that the Jack Hills zircons with Type 2 REE domains were originally precipitated in a crystallizing magma and subsequently altered by circulating hydrothermal fluids, a comparison was made of the characteristics for the Type 2 domains (EA-3) with characteristics of 'hydrothermal zircon' as described by others

from several environments (Tomaschek et al., 2003; Spandler et al., 2004; Hoskin, 2005):

(1) *Texture.* None of the Type 2 (or Type 1) Jack Hills zircon domains have the porous textures reported for hydrothermal zircons from the Boggy Plain Pluton (Hoskin, 2005) or elsewhere (Tomaschek et al., 2003; Spandler et al., 2004).
(2) *Sedimentary transport.* If hydrothermal alteration occurred prior to deposition of these grains in the Jack Hills sediments, it is likely that such porous grains would not have survived sedimentary transport and abrasion; we know of no documented occurrences of detrital zircons of hydrothermal origin.
(3) *CL zoning.* Half of the Type 2 domains display bright intensities or growth zoning in CL [Fig. 1 (j,al,am,an,ao,ap)], unlike the dark CL, unzoned Boggy Plain hydrothermal zircons (Hoskin, 2005). Only grains 01JH54-77 and 01JH60-39 have dark rims in CL (Fig. 1c and p), however, these grains are nearly colorless and optically clear in transmitted light (Cavosie et al., 2004), as opposed to 'murky brown' (Hoskin, 2005).
(4) *Mineral inclusions.* Grains with Type 2 domains have few or no identified mineral inclusions (Cavosie et al., 2004), unlike the hydrothermal zircons described by Tomaschek et al. (2003) and Spandler et al. (2004) that contain numerous inclusions indicative of low-temperature alteration, including celadonite, kaolinite, smectite, thortveitite, and yttrialite.
(5) *Oxygen isotope ratio.* The $\delta^{18}O$ values measured in Type 2 domains (4.6–7.3‰) are consistent with high-temperature magmatic equilibrium between zircon and melt (Cavosie et al., 2005). If these zircons had precipitated from or exchanged with fluids during hydrothermal alteration, variable temperatures and $\delta^{18}O$ (H_2O) values would likely cause considerable scatter in these values. The one exception is grain W74/3-143, a zircon fragment with Type 2 domains that yielded two $\delta^{18}O$ values of 17.7‰ and 18.4‰, significantly higher than those found in any Archean igneous rock (Cavosie et al., 2005; Valley et al., 2005). However, the analyses that yielded the high values overlapped onto cracks, and thus are not considered reliable, in contrast to a magmatic value of $\delta^{18}O = 6.7$‰ from a crack-free area of the same grain.
(6) *HfO_2 content.* Hydrothermal zircons (from the Boggy Plain and elsewhere) contain relatively high HfO_2 values, ranging from 2.8 to 7.6 wt% HfO_2 (Hoskin, 2005). The highest value for HfO_2 in our Jack Hills zircons is 2.0 wt% (from a Type 1 domain), and most analyses yielded significantly lower values, averaging 1.38 ± 0.52 wt% HfO_2 (2 SD) (EA-2).

Fig. 10 displays all of the analyses made in this study on bivariate plots used by Hoskin (2005) to discriminate hydrothermal from magmatic zircon. In the $(Sm/La)_N$ vs. La plot (Fig. 10a), Type 1 analyses cluster in or near the 'magmatic' field (defined by Hoskin, 2005), whereas the Type 2 analyses plot mostly between the 'magmatic' and 'hydrothermal' fields; importantly, none plot within the hydrothermal field on this diagram. Interestingly, the three zircon standards also plot between the two fields, with KIM-5 and 91500 showing an association with Type 1 analyses. A similar result is found for a plot of Ce/Ce* vs. $(Sm/La)_N$ (Fig. 10b), with an overall closer grouping of the Type 1 and Type 2 analyses, however, KIM-5 and CZ3 plot closer to the 'hydrothermal' field, and some Type 2 analyses lie within this field. Fig. 10 shows that our interpretation of Type 1 domains as magmatic is in broad agreement with the classification scheme of Hoskin (2005), and that our criteria for classifying Type 2 domains based on the combination of $La_N > 1$ and $Pr_N > 10$ is useful for identifying zircon domains with possibly non-magmatic REE patterns. However, rare earth element patterns alone appear

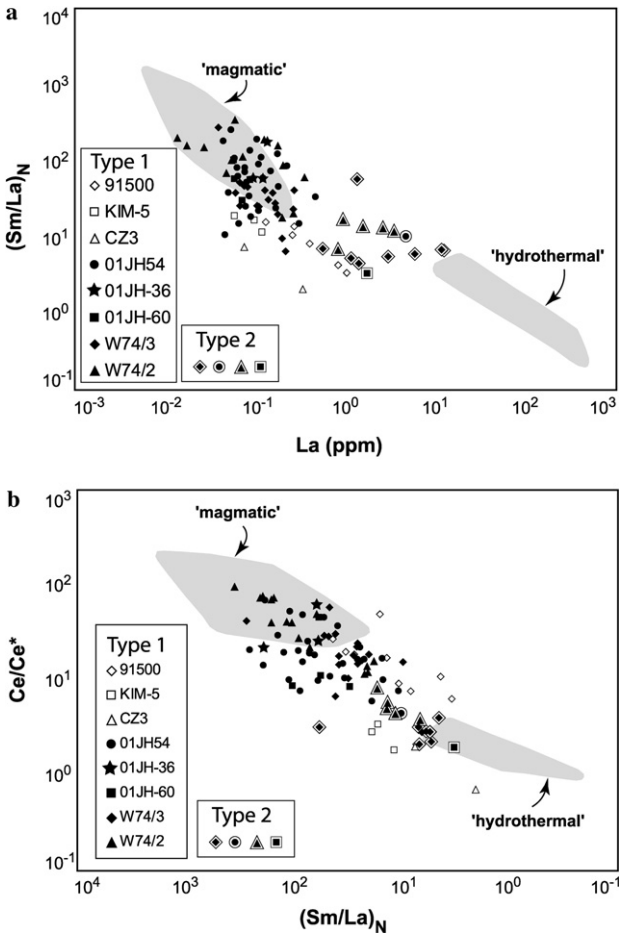

Fig. 10. (a) $(Sm/La)_N$ vs. La (ppm). (b) Ce/Ce* vs. $(Sm/La)_N$. Shaded fields of 'magmatic' and 'hydrothermal' are from Hoskin (2005). Solid symbols are Jack Hills Type 1 analyses. Double-walled symbols are Type 2 analyses. Open symbols are standards.

inadequate for distinguishing hydrothermally precipitated zircon from metamorphic or altered igneous zircons.

Thus, with the exception of LREE enrichment, Type 2 domains in Jack Hills zircons do not have characteristics that resemble previously described 'hydrothermal zircons' formed by a wide range of fluid-assisted processes. Taken together with the constraints provided by oxygen isotope, U–Pb, and Th–U data, the Type 2 domains (where inclusions were not encountered, e.g. EA-4a, -4b) are best interpreted to have formed by alteration of Type 1 zircon, resulting in localized enrichment of LREE in grain areas with radiation damage — this enrichment process may have been mediated by a fluid at very low water:rock ratios. While this conclusion is similar to that reached by Hoskin (2005) and others, we find no evidence for external fluid interaction, which suggests either that the role of fluids in the LREE enrichment process is minor, or that the alteration effects of fluids are so localized that they are not detected in the volume analyzed for $\delta^{18}O$ by ion microprobe (Hoskin, 2005). Thus, to classify these grains as 'hydrothermal' based on the suspicion that a hypothetical fluid may have affected domains much smaller than the 10 μm ion microprobe spot is unwarranted, and would result in additional ambiguity over what constitutes 'true' hydrothermal zircon. We conclude that these are not 'hydrothermal zircons'.

5.4. Metamorphism of Jack Hills zircons

Some of the Jack Hills zircons have clearly experienced post-magmatic thermal events, as evidenced by the number of grains reported with overgrowth ages younger than their respective inherited cores. Three >3900 Ma zircons yielding rim ages ranging from 3730 to 3650 Ma (Cavosie et al., 2004; Crowley et al., 2005), and two additional grains with ca. 3360 Ma rim ages (Cavosie et al., 2004) were attributed to known Archean igneous events in the adjacent Yilgarn Craton. In addition, ca. 3900 Ma rims reported on two >4000 Ma grains record magmatic resorbtion and overgrowth in thermal events older that any exposed rocks in Australia (Maas et al., 1992; Cavosie et al., 2004). Complicated U–Pb age spectra and associated Pb loss from grains with multiple U–Pb analyses have also been cited as evidence for multiple granulite-facies metamorphic events that affected the Jack Hills zircons between 4400 and 4000 Ma (Nelson, 2002, 2004; Nemchin et al., 2006). While the events that caused the formation of younger rims and apparent Pb loss are a matter of speculation, we note that many of the zircons with variable ages and younger rims in the suite reported here preserve oscillatory zoning (e.g. Fig. 1c, d, m, p, s, u, and al), a diagnostic feature of magmatic zircon. Thus despite experiencing complex and largely unknown geologic histories prior to deposition in the Jack Hills sediments, the results of this study demonstrate that these grains contain domains of preserved igneous composition and texture, which record their origin in magmas.

5.5. Trace elements as indicators of protolith

The chondrite normalized REE patterns from Type 1 domains resemble typical 'crustal' zircons from a wide range of igneous rock compositions (Hoskin and Ireland, 2000), and thus do not allow the composition of the protolith to be determined. A multivariate classification and regression tree (CART) developed for identifying the origin of zircons based on trace element composition (Belousova et al., 2002) was used to further investigate the origins of zircons in this study. For the zircon standards, the CART correctly identified KIM-5 as originating from kimberlite, however the classification of both CZ3 and 91500 as originating in carbonatite (EA-1) is not accurate given what is known about the origin of these grains.

For the Jack Hills samples, the CART classified analyses from 37 zircons as originating in granitoid (EA-2). Analyses from seven zircons were classified as originating in dolerite or basalt, although four of these grains also contain domains that yielded analyses that indicated a granitoid origin (EA-2). The remaining five analyses were classified as representing carbonatite, but again, three of these five grains also yielded analyses that indicated an origin in granitoid (EA-2). The CART classification is useful for illustrating general trends in the detrital zircon population, but may not be a reliable identification method for the source of any given zircon, as subtle differences can result in zircons with similar compositions being assigned to different groups. The 11 cases where the CART assigned single zircons to two rock types (e.g. dolerite and granitoid) demonstrate the limitations of the classification scheme.

6. Conclusions

Comparing trace element data from zircon domains previously analyzed for U–Pb and oxygen isotope composition allows preserved magmatic compositions to be identified, and enables an evaluation of the causes of LREE enrichment based on multiple criteria. The trace element data confirm that most of the >3900 Ma detrital zircons from the Jack Hills in our sample set (Type 1) preserve magmatic compositions typical of crustal igneous zircon. Type 2 domains are enriched in LREE relative to Type 1. The observed LREE enrichment is not a record of unusual magma compositions on the early Earth, and is instead likely the result of multiple factors, including inadvertent analysis of sub-surface mineral inclusions in some grains, and localized alteration of radiation damaged parts of grains under low fluid/rock ratio conditions in others. We do not consider Type 2 zircons as 'hydrothermal', as no direct evidence for the presence of fluids was found. The results of this study, which includes data for many of the oldest detrital zircons known, provides additional information on the population of pre-3900 Ma magmatic zircons thus far identified, and adds further support to models that place their origin in

buoyant, quartz-saturated, granitic continent-like crust present on the early Earth.

Acknowledgments

We thank John Craven, Richard Hinton, and Colin Graham for training and assistance on the Edinburgh CAMECA ims-4f, and also for helpful discussions about ion microprobe operation and data reduction, and Nikki Cayzar for assistance with SEM imaging and sample coating in Edinburgh. We thank Noriko Kita for discussions about trace element analysis, Brian Hess for assistance in mounting, polishing, and re-polishing sample mounts to conserve material, John Fournelle for assistance with electron microprobe analyses, and Scott Dhuey for assistance with SEM imaging at the University of Wisconsin. SEM imaging at the University of Wisconsin was conducted at the Center for NanoTechnology at the Synchrotron Radiation Center, which is supported by NSF (DMR-0084402). Support for this work was provided by the NSF (EAR-020734), DOE (93ER14389), and the ARC (DP0211706). The Edinburgh Ion Microprobe Facility is supported by NERC. Paul Hoskin and two anonymous reviewers are thanked for providing constructive comments on the manuscript. Tom Chacko provided valuable editorial suggestions.

Associate editor: Thomas Chacko

Appendix A. Supplementary data

Supplementary data associated with this article can be found, in the online version, at doi:10.1016/j.gca.2006.08.011.

References

Amelin, Y., Lee, D.-C., Halliday, A.N., Pidgeon, R.T., 1999. Nature of Earth's earliest crust from hafnium isotopes in single detrital zircons. *Nature* **399**, 252–255.

Belousova, E.A., Griffin, W.L., Pearson, N.J., 1998. Trace element composition and cathodoluminescence properties of southern African kimberlitic zircons. *Min. Mag.* **62**, 355–366.

Belousova, E.A., Griffin, W.L., O'Reilly, S.Y., Fisher, N.I., 2002. Igneous zircon: trace element composition as an indicator of source rock type. *Contrib. Mineral. Petrol.* **143**, 602–622.

Bingen, B., Austrheim, H., Whitehouse, M.J., Davis, W.J., 2004. Trace element signature and U-Pb geochronology of eclogite-facies zircon, Bergen Arcs, Caledonides of W. Norway. *Contrib. Mineral. Petrol.* **147**, 671–683.

Bowring, S.A., Williams, I.S., 1999. Priscoan (4.00–4.03 Ga) orthogneisses from northwestern Canada. *Contrib. Mineral. Petrol.* **134**, 3–16.

Cavosie, A.J., Wilde, S.A., Liu, D., Weiblen, P.W., Valley, J.W., 2004. Internal zoning and U–Th–Pb chemistry of Jack Hills detrital zircons: a mineral record of early Archean to Mesoproterozoic (4348–1576 Ma) magmatism. *Precambrian Res.* **135**, 251–279.

Cavosie, A.J., Valley, J.W., Wilde, S.A., EIMF, 2005. Magmatic $\delta^{18}O$ in 4400–3900 Ma detrital zircons: a record of the alteration and recycling of crust in the Early Archean. *Earth Planet. Sci. Lett.* **235**, 663–681.

Compston, W., Pidgeon, R.T., 1986. Jack Hills, evidence of more very old detrital zircons in Western Australia. *Nature* **321**, 766–769.

Crowley, J.L., Myers, J.S., Sylvester, P.J., Cox, R.A., 2005. Detrital zircon from the Jack Hills and Mount Narryer, Western Australia: evidence for diverse >4.0 Ga source rocks. *J. Geol.* **113**, 239–263.

Finch, J.R., Hanchar, J.M., 2003. Structure and chemistry of zircon and zircon-group minerals. In: Hanchar, J.M., Hoskin, P.W.O. (Eds.), Zircon. *Rev. Mineral. Geochem.* 53, 1–25.

Finch, J.R., Hanchar, J.M., Hoskin, P.W.O., Burns, P.C., 2001. Rare-earth elements in synthetic zircon: Part 2. A single-crystal X-ray study of xenotime substitution. *Am. Mineral.* **86**, 681–689.

Froude, D.O., Ireland, T.R., Kinny, P.D., Williams, I.S., Compston, W., Williams, I.R., Myers, J.S., 1983. Ion microprobe identification of 4100–4200 Myr-old terrestrial zircons. *Nature* **304**, 616–618.

Hanchar, J.M., Finch, J.R., Hoskin, P.W.O., Watson, E.B., Cherniak, D.J., Mariano, A.N., 2001. Rare earth elements in synthetic zircon: Part 1. Synthesis, and rare earth element and phosphorus doping. *Am. Mineral.* **86**, 667–680.

Harrison, T.M., Blichert-Toft, J., Muller, W., Albarede, F., Holden, P., Mojzsis, S.J., 2005. Heterogeneous Hadean hafnium: evidence of continental crust at 4.4 to 4.5 Ga. *Science* **310**, 1947–1950.

Hinton, R.W., 1996. Comparison of yttrium and holmium concentrations: natural vs. analytical variability. *J. Conf. Abst.* **1** (1), 258.

Hinton, R.W., Upton, B.G.J., 1991. The chemistry of zircon: variations within and between large crystals from syenite and alkali basalt xenoliths. *Geochim. Cosmochim. Acta* **55**, 3287–3302.

Hinton, R.W., Macdonald, R., McGarvie, D.W., Tindle, A., Harley, S.L., 2003. The possible role of hydrogen in the substitution of rare earth elements into zircon. *Geophys. Res. Abst.* **5**, 5968.

Hoskin, P.W.O., 1998. Minor and trace element analysis of natural zircon ($ZrSiO_4$) by SIMS and laser ablation ICPMS: a consideration and comparison of two broadly competitive techniques. *J. Trace Microprobe Techniques* **16**, 301–326.

Hoskin, P.W.O., 2005. Trace-element composition of hydrothermal zircon and the alteration of Hadean zircon from the Jack Hills, Australia. *Geochim. Cosmochim. Acta* **69**, 637–648.

Hoskin, P.W.O., Black, L.P., 2000. Metamorphic zircon formation by solid-state recrystallization of protolith igneous zircon. *J. Metamorphic Geol.* **18**, 423–439.

Hoskin, P.W.O., Ireland, T.R., 2000. Rare earth element chemistry of zircon and its use as a provenance indicator. *Geology* **28**, 627–630.

Hoskin, P.W.O., Schaltegger, U., 2003. The composition of zircon and igneous and metamorphic petrogenesis. In: Hanchar, J.M., Hoskin, P.W.O. (Eds.), Zircon. *Rev. Mineral. Geochem.* 53, 27–55.

Hoskin, P.W.O., Kinny, P.D., Wyborn, D., Chappell, B.W., 2000. Identifying accessory mineral saturation during differentiation in granitoid magmas: an integrated approach. *J. Petrol.* **41**, 1365–1396.

Iizuka, T., Horie, K., Komiya, T., Maruyama, S., Hirata, T., Hidaka, H., Windley, B.F., 2006. 4.2 Ga zircon xenocryst in an Acasta gneiss from northwestern Canada: evidence for early continental crust. *Geology* **34**, 245–248.

Ireland, T.R., Wlotzka, F., 1992. The oldest zircons in the solar system. *Earth Planet. Sci. Lett.* **109**, 1–10.

Maas, R., Kinny, P.D., Williams, I.S., Froude, D.O., Compston, W., 1992. The Earth's oldest known crust: a geochronological and geochemical study of 3900–4200 Ma old detrital zircons from Mt. Narryer and Jack Hills, Western Australia. *Geochim. Cosmochim. Acta* **56**, 1281–1300.

McDonough, W.F., Sun, S.-S., 1995. The composition of the Earth. *Chem. Geol.* **120**, 223–253.

Mojzsis, S.J., Harrison, T.M., Pidgeon, R.T., 2001. Oxygen-isotope evidence from ancient zircons for liquid water at the Earth's surface 4300 Myr ago. *Nature* **409**, 178–181.

Nasdala, L., Reiners, P.W., Garver, J.I., Kennedy, A.K., Stern, R.A., Balan, E., Wirth, R., 2004. Incomplete retention of radiation damage in zircon from Sri Lanka. *Am. Mineral.* **89**, 219–231.

Nelson, D.R., 2002. Hadean Earth crust: microanalytical investigation of 4.4 to 4.0 Ga zircons from Western Australia. *Geochim. Cosmochim. Acta* **66**, A549, abstract.

Nelson, D.R., 2004. The early Earth, Earth's formation and first billion years. In: Eriksson, P.G. et al. (Eds.), *The Precambrian Earth: Tempo and Events*. Elsevier, Amsterdam, pp. 3–27.

Nelson, D.R., Robinson, B.W., Myers, J.S., 2000. Complex geological histories extending for $\geqslant$4.0 Ga deciphered from xenocryst zircon microstructures. *Earth Planet. Sci. Lett.* **181**, 89–102.

Nemchin, A.A., Pidgeon, R.T., Whitehouse, M.J., 2006. Re-evaluation of the origin and evolution of >4.2 Ga zircons from the Jack Hills metasedimentary rocks. *Earth Planet. Sci. Lett.* **244**, 218–233.

Pearce, J.G., Perkins, W.T., Westgate, J.A., Gorton, M.P., Jackson, S.E., Neal, C.R., Chenery, S.P., 1997. A compilation of new and published major and trace element data for NIST SRM 610 and NIST SRM 612 glass reference materials. *Geostandards Newslett.* **21**, 115–144.

Peck, W.H., Valley, J.W., Wilde, S.A., Graham, C.M., 2001. Oxygen isotope ratios and rare earth elements in 3.3 to 4.4 Ga zircons: ion microprobe evidence for high $\delta^{18}O$ continental crust and oceans in the Early Archean. *Geochim. Cosmochim. Acta* **65**, 4215–4229.

Pidgeon, R.T., Furfaro, D., Kennedy, A.K., Nemchin, A.A., Van Bronswjk, W., 1994. Calibration of zircon standards for the Curtin SHRIMP II. ICOG 8. *US Geol. Surv. Circular* **1107**, 251, abstract.

Rayner, N., Stern, R.A., Carr, S.D., 2005. Grain-scale variations in trace element composition of fluid-altered zircon, Acasta Gneiss Complex, northwestern Canada. *Contrib. Mineral. Petrol.* **148**, 721–734.

Rubatto, D., 2002. Zircon trace element geochemistry: partitioning with garnet and the link between U–Pb ages and metamorphism. *Chem. Geol.* **184**, 123–138.

Spandler, C., Hermann, J., Rubatto, D., 2004. Exsolution of thortveitite, yttrialite, and xenotime during low-temperature recrystallization of zircon from New Caledonia, and their significance for trace element incorporation in zircon. *Am. Mineral.* **89**, 1795–1806.

Speer, J.A., 1982. Zircon. Orthosilicates. *Rev. Mineral.* **5**, 67–112.

Spetsius, Z.V., Belousova, E.A., Griffin, W.L., O'Reilly, S.Y., Pearson, N.J., 2002. Archean sulfide inclusions in Paleozoic zircon megacrystals from the Mir kimberlite, Yakutia: implications for the dating of diamonds. *Earth Planet. Sci. Lett.* **199**, 111–126.

Tomaschek, F., Kennedy, A.K., Villa, I.M., Lagos, M., Ballhaus, C., 2003. Zircons from Syros, Cyclades, Greece—recrystallization and mobilization of zircon during high-pressure metamorphism. *J. Petrol.* **44**, 1977–2002.

Turner, G., Harrison, T.M., Holland, G., Mojzsis, S.J., Gilmour, J., 2004. Extinct ^{244}Pu in ancient zircons. *Science* **306**, 89–91.

Valley, J.W., 2003. Oxygen isotopes in zircon. In: Hanchar, J.M., Hoskin, P.W.O. (Eds.), Zircon. *Rev. Mineral. Geochem.* 53, 343–385.

Valley, J.W., Kinny, P.D., Schulze, D.J., Spicuzza, M.J., 1998. Zircon megacrysts from kimberlite: oxygen isotope variability among mantle melts. *Contrib. Mineral. Petrol.* **133**, 1–11.

Valley, J.W., Peck, W.H., King, E.M., Wilde, S.A., 2002. A cool early Earth. *Geology* **30**, 351–354.

Valley, J.W., Lackey, J.S., Cavosie, A.J., Clechenko, C.C., Spicuzza, M.J., Basei, M.A.S., Bindeman, I.N., Ferreira, V.P., Sial, A.N., King, E.M., Peck, W.H., Sinha, A.K., Wei, C.S., 2005. 4.4 billion years of crustal maturation: oxygen isotope ratios of magmatic zircon. *Contrib. Mineral. Petrol.* **150**, 561–580.

Valley, J.W., Cavosie, A.J., Fu, B., Peck, W.H., Wilde, S.A., 2006. Comment on "Heterogeneous Hadean Hafnium: Evidence of Continental Crust at 4.4 to 4.5 Ga". *Science* **312**, 1139a.

Watson, E.B., Harrison, T.M., 2005. Zircon thermometer reveals minimum melting conditions on earliest Earth. *Science* **308**, 841–844.

Whitehouse, M.J., Kamber, B.S., 2002. On the overabundance of light rare earth elements in terrestrial zircons and its implications for Earth's earliest magmatic differentiation. *Earth Planet. Sci. Lett.* **6442**, 1–14.

Whitehouse, M.J., Platt, J.P., 2003. Dating high-grade metamorphism-constraints from rare-earth elements in zircon and garnet. *Contrib. Mineral. Petrol.* **145**, 61–74.

Wiedenbeck, M., Hanchar, J.M., Peck, W.H., Sylvester, P., Valley, J.W., Whitehouse, M., Kronz, A., Morishita, Y., Nasdala, L., Fiebig, J., Franchi, I., Girard, J.-P., Greenwood, R.C., Hinton, R., Kita, N., Mason, P.R.D., Norman, M., Ogasawara, M., Piccoli, P.M., Rhede, D., Satoh, H., Schulz-Dobrick, B., Skar, O., Spicuzza, M.J., Terada, K., Tindle, A., Togashi, S., Vennemann, T., Xie, Q., Zheng, Y.-F., 2004. Further characterization of the 91500 zircon crystal. *Geostandards Geoanalytical Res.* **28**, 9–39.

Wilde, S.A., Valley, J.W., Peck, W.H., Graham, C.M., 2001. Evidence from detrital zircons for the existence of continental crust and oceans on the Earth 4.4 Gyr ago. *Nature* **409**, 175–178.

Wu, F.Y., Yang, Y.H., Xie, L.W., Yang, J.H., Xu, P., 2006. Hf isotopic compositions of the standard zircons and baddeleyites used in U–Pb geochronology. *Chem. Geol.* **232**. doi:10.1016/j.chemgeo.2006.05.003.

Wyche, S., Nelson, D.R., Riganti, A., 2004. 4350–3130 Ma detrital zircons in the Southern Cross Granite-Greenstone Terrane, Western Australia: implications for the early evolution of the Yilgarn Craton. *Aust. J. Earth Sci.* **51**, 31–45.